University of Wollongong

Research Online

1-1-2013

Critical current density: Measurements vs. reality

Alexey V. Pan
University of Wollongong, pan@uow.edu.au

Igor Golovchanskiy
University of Wollongong, ig684@uowmail.edu.au

Sergey Fedoseev
University of Wollongong, sergey@uow.edu.au

Recommended Citation

Critical current density: Measurements vs. reality

Abstract

Different experimental techniques are employed to evaluate the critical current density (Jc), namely transport current measurements and two different magnetisation measurements forming quasi-equilibrium and dynamic critical states. Our technique-dependent results for superconducting YBa 2Cu3O7 (YBCO) film and MgB2 bulk samples show an extremely high sensitivity of Jc and associated interpretations, such as irreversibility fields and Kramer plots, which lose meaning without a universal approach. We propose such approach for YBCO films based on their unique pinning features. This approach allows us to accurately recalculate the magnetic-field-dependent Jc obtained by any technique into the Jc behaviour, which would have been measured by any other method without performing the corresponding experiments. We also discovered low-frequency-dependent phenomena, governing flux dynamics, but contradicting the considered ones in the literature. The understanding of these phenomena, relevant to applications with moving superconductors, can clarify their dramatic impact on the electric-field criterion through flux diffusivity and corresponding measurements. © Copyright EPLA, 2013.

epl draft

Critical current density: measurements versus reality

A. V. Pan*, I. A. Golovchanskiy and S. A. Fedoseev

Institute for Superconducting and Electronic Materials, University of Wollongong, Northfields Avenue, Wollongong, NSW 2522, Australia
* *pan@uow.edu.au*

Abstract –Different experimental techniques are employed to evaluate the critical current density (J_c), namely transport current measurements and two different magnetization measurements forming quasi-equilibrium and dynamic critical states. Our technique-dependent results for superconducting $YBa_2Cu_3O_7$ (YBCO) film and MgB_2 bulk samples show extremely high sensitivity of J_c and associated interpretations, such as irreversibility fields and Kramer plots, which lose meaning without an universal approach. We propose such approach for YBCO films based on their unique pinning features, which allow us to recalculate vortex behaviour affected by the measurements into the real J_c independent of measurement techniques. We also discovered low frequency-dependent phenomena, governing flux dynamics, but contradicting to the considered ones in the literature. The understanding of these phenomena, relevant to applications with moving superconductors, can clarify their dramatic impact on the electric field criterion through flux diffusivity and corresponding measurements.

Superconductivity is one of the most fascinating and promising phenomena in nature. It offers benefits of no energy losses in electricity handling due to the absence of resistance below the critical temperature, as well as variety of quantum phenomena, e.g. magnetic flux quanta (vortices) whose immobilization is the key to achieving zero resistance [1] in practical superconductors.

A lot of attempts to describe critical current density (J_c) behaviour as a function temperature (T) and applied magnetic field (B_a) have been made [2–7]. However, these descriptions in practical superconductors, particularly in high temperature superconductors (HTS), have always been limited due to the complexity of the problem. Moreover, the critical state of the superconductors cannot be described as a unique physical state [1, 2, 8]. Indeed, vortex creep in superconductors affects the balance of the Lorentz-pinning forces, generating electrical fields and enabling energy losses [2,8]. The magnitude of these electric fields leads to inconsistent results measured by different experimental techniques (transport current, equilibrium and dynamic magnetic measurements, etc.) [9,10] and, as a result, to their possible misinterpretations. Although the overall situation is far from being critical for practical applications [11], a unified standardisation of various measurements and, more importantly, their interpretations [12] would help to avoid physical misconceptions and make an accurate match between applications and practical availability.

In this work, we combined the results obtained for different experimental techniques with our quantitative pinning model [5, 6, 13] incorporating the electric field criterion (E_{cr}), in order to show the significant extent of existing inconsistencies, as well as to understand them and unify the outcome from different experimental techniques and corresponding interpretations.

In Fig. 1(a), the experimental results (symbols) obtained by different measurement techniques are shown for *the same* HTS $YBa_2Cu_3O_7$ (YBCO) high quality thin film, which is 400 nm thick grown by pulsed laser deposition [14, 15] on a 5×5 mm^2 $SrTiO_3$ substrate. We employ (i) standard home-built four-probe DC transport current measurements with two different electric field criteria $E_{cr} = 10^{-4}$ V/m and 10^{-3} V/m; (ii) the semi-equilibrium MPMS (SQUID) magnetization measurements with the field swept from one set-point to another and measurements taken at each set-point with the field being kept constant; and (iii) non-equilibrium PPMS vibrating sample magnetization (VSM) measurements with the field
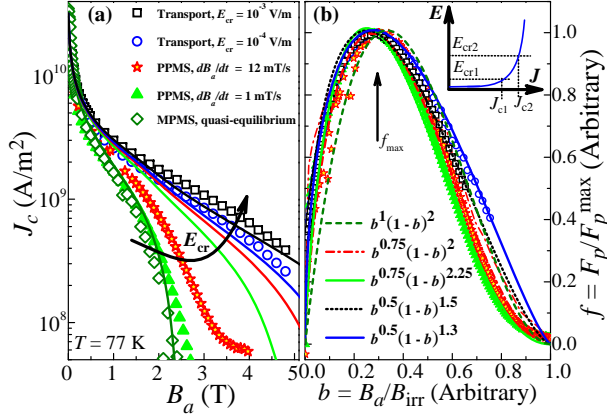
Fig. 1: (a) Transport current measurements with different electric field criteria, equilibrium (denoted as MPMS) magnetization measurements, and non-equilibrium (denoted as PPMS) magnetization measurements taken with different magnetic field sweep rates for the same YBCO film. The solid lines are the model fits. (b) Corresponding Kramer plots with their fits. The inset shows schematic of how two different E_{cr} lead to two J_c values for the same $E-J$ curve.

being swept with the constant dB_a/dt equal to 1 mT/s and 12 mT/s, while measurements are taken. The DC magnetic field is always applied perpendicular to the film plane. The $J_c(B_a, T)$ dependences for MPMS and PPMS have been obtained from the width of the magnetization loops $\Delta M(B_a, T) = |M^+| + |M^-|$, using the critical state model: $J_c = 2\Delta M/[w_p(1 - w_p/3l_p)]$ in A/m^2, where w_p and l_p are respectively width and length of the samples measured. After carrying out all the magnetisation measurements, the film was patterned into a bridge of 16 μm wide and 320 μm long by employing optical photolithography.

There is a striking difference between the J_c curves measured for the same *one* film, which should have been identical. It would be sufficient to mention more than 4-fold difference for the irreversibility field (B_{irr}) determined at $J_c = 5 \times 10^7$ A/m^2. This result is often neglected in determining, for example, pinning mechanisms or superconducting parameters. The irreversibility field is known as the line of a constant diffusivity $D(T, B_a) = \rho(T, B_a)/\mu_0$, indicating vortex depinning [16]. It is accompanied by the onset of resistivity [17] or electric field, whose detection criterion (E_{cr}) may vary in the case of transport current measurements and magnetization measurements. In the latter case, $E_{cr} = s_p(dB_a/dt)$ is determined by the sweep rate of the magnetic field (dB_a/dt) and the effective transverse size (s_p) of the sample [18].

The practically important current-carrying performance is usually determined by four-probe transport current measurements with the criterion of $E_{cr} = 10^{-4}$ V/m. Lower (and higher) E_{cr} may be used [12,19]. Which measurements (or criteria) provide the most reliable and vi-

able result from practical and physical point of view? On one hand, the transport measurement may provide a most practical description for the current flow. On the other hand, it is less sensitive compared to, for example, magnetization measurements. A lower sensitivity means a larger E_{cr}, as schematically depicted in the inset to Fig. 1(b), and hence assumes more substantial flux motion (and corresponding energy dissipation) [1,2].

The difference in understanding the pinning mechanisms relying on different E_{cr} can be significant [12]. Without going into details of various interpretations for J_c and B_{irr} available in the literature, we employ well-known Kramer plots [20] of the normalized pinning force $F_p/F_p^{max} = f = b^p(1 - b)^q$ to illustrate it ($b = B_a/B_{irr}$; F_p^{max} is the maximum pinning force obtained in the $F_p(B_a)$ dependence with $F_p = J_c B_a$; p and q are the parameters related to pinning mechanisms [20–24]).

In Fig. 1(b), the $f(b)$ Kramer plots are shown with their respective fitting curves. We obtain $f_{max} = 0.2$ to 0.3, indicating the expected core pinning [20,22] for the YBCO films. However, we obtain significant scattering in $p \simeq 0.5$ to 1 and $q \simeq 1.3$ to 2. This certainly leads to misinterpretations (such as "physics of one measurement"), because the same analysis of the same property measured by different type of instruments for one sample should provide one self-consistent explanation, which is obviously not the case.

To understand this inconsistent behaviour, we have calculated the $J_c(B_a)$ curves for the YBCO film using our model of vortex pinning on edge dislocations [5,15], which also includes flux creep and electric field criterion [13] as follows

$$J(B_a, T) \propto \text{asinh}\left[\alpha \frac{E_{cr}}{B_a^{3/2}} \exp\left(\beta \frac{n_p}{n_v}(B_a, T)\right)\right], \quad (1)$$

where α and β are material related parameters, and n_p/n_v is the so-called accommodation function, which determines the ratio of the pinned vortices (n_p) to the total number of vortices (n_v) depending on particular defect structure in YBCO films. The result of the calculation is shown as solid lines in Fig. 1(a). In fact, we have initially fitted the model $J_c(B_a, T, E_{cr}, U_p)$ to the MPMS results [25], which, along with other fitting parameters, gave us $E_{cr} \simeq 10^{-11}$ V/m. By fixing the fitting parameters and changing only E_{cr} (corresponding to the criterion used for each type of measurements), we can accurately reproduce the experimental curves for the transport current measurements. However, the PPMS results do not correspond to the model curves obtained with $E_{cr} \simeq s_p(dB_a/dt)$ [Fig. 1(a)].

To clarify this problem, we have identified the measurement frequency of the PPMS VSM as the parameter affecting the measurement results, which has never been considered in the literature. Hence, we have measured our film in PPMS with different VSM frequencies leaving all the other parameters unchanged (including $dB_a/dt = 5$ mT/s). In
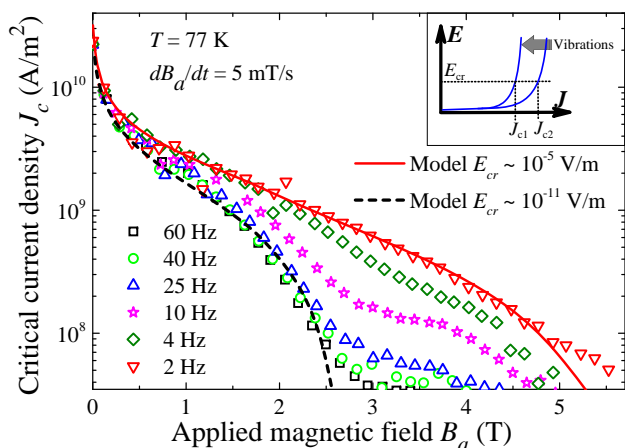
Fig. 2: Frequency dependence of YBCO films measured in PPMS with the model curves for two limiting frequency cases. The inset shows the effect of vibration on a $E - J$ curve.

Fig. 3: The $B_{irr}(E_{cr})$ curve obtained from the model calculation using the parameters for the YBCO films obtained from the fit to MPMS curve [13, 25], while varying only E_{cr}. The shaded areas indicate E_{cr} for each technique employed without taking into account vibrations.

Fig. 2, one sees another remarkable difference in the results exhibiting not only increase in B_{irr} by a factor of 2.5 with decreasing measurement frequency (which can affect Kramer plots), but also strongly changing regimes of vortex pinning and dynamics. For example, a clear crossover between two different vortex pinning/flow regimes can be seen as non-monotonous $J_c(B_a)$ behaviour, which is pronounced the most for the J_c curves measured at 10 Hz and 25 Hz above 2.5 T.

Fitting the model curves to the results obtained, we find that E_{cr} can vary over the 6 (six) orders of magnitude as indicated by the lines for the lowest (2 Hz) to highest (60 Hz) frequency used, corresponding to $E_{cr} \simeq 10^{-5}$ V/m and 10^{-11} V/m. Thus, it is no longer surprising that we could not fit the $J_c(B_a)$ results measured by PPMS at the factory set default frequency of 40 Hz (Fig. 1). Obviously, the frequency strongly affects the flux dynamics and energy dissipation as schematically indicated in the inset to Fig. 2.

In general, the range of E_{cr} for each of three techniques employed in this work is shown in Fig. 3 by rectangular shadings. In fact, the E_{cr} ranges can be much broader, it depends on benchmark choice, noise threshold, equipment sensitivity and resolution, experiment environment (stability), and even sample properties. The $B_{irr}(E_{cr})$ dependence shown in Fig. 3 is obtained from our model [13] $J_c(B_a, T, E_{cr}, U_p)$ using the parameters for the YBCO film measured in a similar fashion as the fitting curves in Fig. 2.

In Fig. 4(a), the similar frequency dependent PPMS measurements are shown for MgB_2 *bulk* superconductor (being $1 \times 2 \times 3$ mm^3) fabricated as described in our previous works [24,26,27]. MgB_2 is known to exhibit different vortex pinning behaviour to HTS [11, 28], hence it would be expected to behave differently upon changing PPMS frequency. It does behave differently to the YBCO film
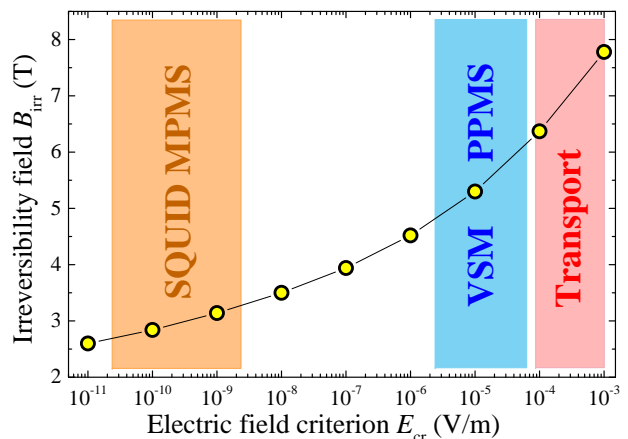
(compare to Fig. 2), but still demonstrates a frequency dependence at high fields. The frequency increase from 2 Hz to 50 Hz leads to the B_{irr} decrease by 1.3 T, which leads to notable changes in pinning description in the Kramer plots (Fig. 4b). Note the much smaller $J_c = 10^5$ A/m^2 criterion used for determining B_{irr} than that for the YBCO film. This has become possible due to much larger MgB_2 sample dimensions, which are known to affect B_{irr} as well [29–31].

In Fig. 5, the magnetization relaxation measurements are shown for two different measurement frequencies. The higher frequency of 50 Hz exhibits enhanced relaxation, which is equivalent to the magnetization J_c measurements at a slower field sweep rate (dB_a/dt), corresponding to a lower E_{cr} (Fig. 1a). The frequency dependence relevant to the relaxation implies that for conventional low temperature superconductors with $U_p >> k_B T$ and its negligible relaxation effects, the PPMS measurement frequency is of marginal significance.

More detailed flux dynamics at low frequencies will be published elsewhere, which may be of importance to rotating superconducting systems, such as motors, fly-wheels, power generators (e.g. wind-mills), etc. In this work, we only note that this low-frequency effect has not been reported. It contradicts to (i) the enhancement of B_{irr} and T_{irr} in increasing frequencies from as low as 20 Hz [32] to the so-called depinning frequency [33–35] due to the increasing immobility of vortices as the response to the increasing frequency; and to (ii) the onset of dissipations above the depinning frequency [36] explained within the mean-field model [37]. In addition, the flux diffusion and magnetization relaxation also indicate a different origin to the so-called Paramagnetic effect measured in MPMS, where temperature and field inhomogeneities experienced by samples during measurements induced highly inhomo-
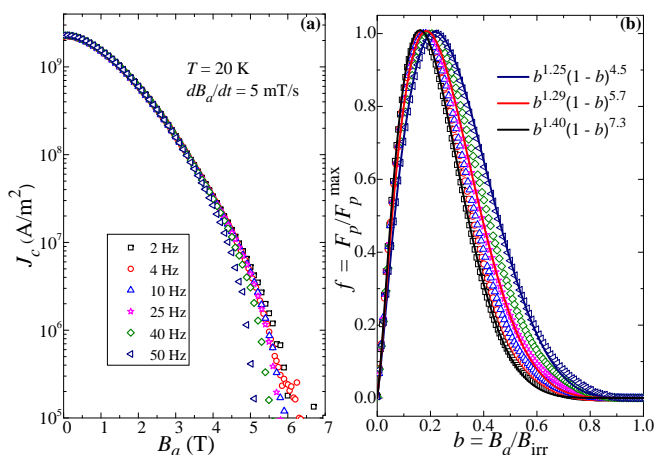
Fig. 4: (a) The frequency dependence of MgB$_2$ superconductor measured in PPMS. (b) Corresponding Kramer plots with their fitting curves.

Fig. 5: The effect of YBCO film vibrations in PPMS. The magnetization decays faster at the higher measurement frequency of 50 Hz.

geneous spatial redistribution of vortices [38].

In summary, we demonstrated how the measurements nominally providing "the same" information can strongly influence its interpretation, J_c, and even the behaviour of the superconductors on the example of YBCO film and MgB$_2$ bulk samples affected by thermal fluctuations. We were able to offer a consistent interpretation of J_c measurements for YBCO films independent of experimental techniques. We also discovered vortex pinning regimes contradicting to the behaviour described in the literature.

$* * *$

REFERENCES

[1] D. A. Huse, M. P. A. Fisher, D. S. Fisher, *Nature*, **358** (1992) 553.

[2] P. Anderson and Y. Kim, *Rev. Mod. Phys.*, **36** (1964) 39.

[3] J. R. Clem, B. Bumble, S. I. Raider, W. J. Gallagher, Y. C. Shih,, Phys. Rev. B 35, 6637 (1987).

[4] E. Mezzetti, R. Gerbaldo, G. Ghigo, L. Gozzelino, B. Minetti, C. Camerlingo, A. Monaco, G. Cuttone, A. Rovelli, *Phys. Rev. B*, **60** (1999) 7623.

[5] V. Pan, Y. Cherpak, V. Komashko, S. Pozigun, C. Tretiachenko, A. Semenov, E. Pashitskii, A. V. Pan, *Phys. Rev. B*, **73** (2006) 054508.

[6] A. V. Pan, S. V. Pysarenko, S. X. Dou, *IEEE Trans. Appl. Supercond.*, **19** (2009) 3391.

[7] D. Dew-Hughes, *Cryogenics*, **28** (1988) 674.

[8] Y. Yeshurun, A. P. Malozemoff, and A. Shaulov, *Rev. Mod. Phys.*, **68** (1996) 911.

[9] A. A. Zhukov, J. P. Ströbel, P. Kummeth, M. Kraus, S. Peechs, W. Schindler, I. Khasanow, H.-W. Neumüller, G. Saemann-Ischenko, A. A. Yarygin, S. I. Krasnosvobodtzev, *Cryogenics*, **33** (1993) 142.
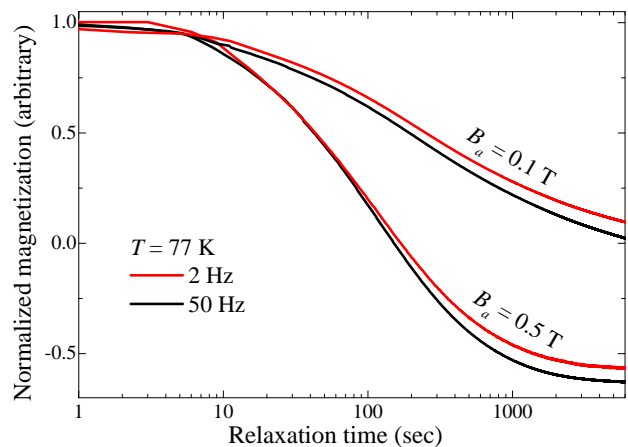
[10] Ö. Polat, J. W. Sinclair, Y. I. Zuev, J. R. Thompson, D. K. Christen, S. W. Cook, D. Kumar, Y. Chen, V. Selvamanickam, *Phys. Rev. B*, **84** (2011) 024519.

[11] D. C. Larbalestier, A. Gurevich, D. M. Feldmann, A. Polyanskii, *Nature*, **414** (2001) 368.

[12] V. F. Solovjov, V. M. Pan, and H. C. Freyhardt, *Phys. Rev. B*, **50** (1994) 13724.

[13] I. A. Golovchanskiy, A. V. Pan, S. X. Dou, *Supercond. Sci. Technol.*, **24** (2011) 105020.

[14] A. V. Pan, S. Pysarenko, S. X. Dou, *Appl. Phys. Lett.*, **88** (2006) 232506.

[15] A. V. Pan, S. V. Pysarenko, D. Wexler, S. Rubanov, S. X. Dou, *IEEE Trans. Appl. Supercond.*, **17** (2007) 3585.

[16] P. Esquinazi, *J. Low Temp. Phys.*, **85** (1991) 139.

[17] A. V. Pan, F. Ciovacco, P. Esquinazi, M. Lorenz, *Phys. Rev. B*, **60** (1999) 4293.

[18] E. H. Brandt, *Phys. Rev. B*, **52** (1995) 15442.

[19] D. M. J. Taylor, D. P. Hampshire, *Supercond. Sci. Technol.*, **18** (S297) 2005.

[20] E. J. Kramer, *J. Appl. Phys.*, **44** (1973) 1360; D. Dew-Hughes, *Phil. Mag.*, **30** (1974) 293.

[21] S. Oh, H. Choi, C. Lee, S. Lee, J. Yoo, D. Youm, H. Yamada, H. Yamasaki, *J. Appl. Phys.*, **102** (2007) 043904.

[22] C. V. Varanasi, P. N. Barnes, and J. Burke, *Supercond. Sci. Technol.*, **20** (2007) 1071.

[23] D. C. Larbalestier, L. D. Cooley, M. O. Rikel, A. A. Polyanskii, J. Jiang, S. Patnaik, X. Y. Cai, D. M. Feldmann, A. Gurevich, A. A. Squitieri, et al., *Nature*, **410** (2001) 186.

[24] O. V. Shcherbakova, A. V. Pan, J. L. Wang, A. V. Shcherbakov, S. X. Dou, D. Wexler, E. Babić, M. Jerčinović, O. Husnjak, *Supercond. Sci. Technol.*, **21** (2008) 015005.

[25] I. A. Golovchanskiy, A. V. Pan, S. A. Fedoseev, O. V. Shcherbakova, S. X. Dou, *Physica C*, **479** (2012) 151.

[26] O. V. Shcherbakova, A. V. Pan, D. Wexler, S. X.

Dou, *IEEE Trans. Appl. Supercond.*, **17** (2007) 2790.

[27] S. Zhou, A. V. Pan, J. Horvat, M. J. Qin, and H. K. Liu, *Supercond. Sci. Technol.*, **17** (2004) S528.

[28] A. V. Pan, S. X. Dou, *Phys. Rev. B*, **73** (2006) 052506.

[29] E. H. Brandt, *Phys. Rev. Lett.*, **68** (1992) 3769.

[30] Q. Li, M. Suenaga, Q. Li, and T. Freltoft, *Appl. Phys. Lett.*, **64** (1994) 250.

[31] J. Horvat, S. Soltanian, A. V. Pan, X. L. Wang, *J. Appl. Phys.*, **96** (2004) 4342.

[32] K. Xu, X. Wu, P. Pan, *Appl. Phys. Lett.*, **95** (2009) 072502.

[33] A. P. Malozemoff, T. K. Worthington, Y. Yeshurun, and F. Holtzberg, *Phys. Rev. B*, **38** (1988) 7203.

[34] K. H. Müller, *Physica C*, **168** (1990) 585.

[35] H. K. Olsson, R. H. Koch, R. P. Robertazzi, *Phys. Rev. Lett.*, **66** (1991) 2661.

[36] J. Owliaei, S. Sridhar, J. Talvacchio, *Phys. Rev. Lett.*, **1992** (69) 3366.

[37] M. W. Coffey, J. R. Clem, *Phys. Rev. Lett.*, **67** (1991) 386.

[38] D. A. Luzhbin, A. V. Pan, V. A. Komashko, V. S. Flis, V. M. Pan, S. X. Dou, P. Esquinazi, *Phys. Rev. B*, **69** (2004) 024506.